Accepted Manuscript

Synthesis, molecular structure, and metabolic stability of new series of *N′*-(2-alkylthio-4-chloro-5-methylbenzenesulfonyl)-1-(5-phenyl-1*H*-pyrazol-1-yl)amidine as potential anti-cancer agents

Aneta Pogorzelska, Jarosław Sławiński, Anna Kawiak, Beata Żołnowska, Jarosław Chojnacki, Grzegorz Stasiłojć, Szymon Ulenberg, Krzysztof Szafrański, Tomasz Bączek

PII: S0223-5234(18)30523-3

DOI: 10.1016/j.ejmech.2018.06.032

Reference: EJMECH 10502

To appear in: *European Journal of Medicinal Chemistry*

Received Date: 16 March 2018

Revised Date: 28 May 2018

Accepted Date: 12 June 2018

Please cite this article as: A. Pogorzelska, Jarosł. Sławiński, A. Kawiak, B. Żołnowska, Jarosł. Chojnacki, G. Stasiłojć, S. Ulenberg, K. Szafrański, T. Bączek, Synthesis, molecular structure, and metabolic stability of new series of *N′*-(2-alkylthio-4-chloro-5-methylbenzenesulfonyl)-1-(5-phenyl-1*H*-pyrazol-1-yl)amidine as potential anti-cancer agents, *European Journal of Medicinal Chemistry* (2018), doi: 10.1016/j.ejmech.2018.06.032.

Synthesis, molecular structure, and metabolic stability of new series of *N'*-(2-alkylthio-4-chloro-5-methylbenzenesulfonyl)-1-(5-phenyl-1*H*-pyrazol-1-yl)amidine as potential anti-cancer agents, Aneta Pogorzelska, Jarosław Sławiński, Anna Kawiak, Beata Żołnowska, Jarosław Chojnacki, Grzegorz Stasiłojć, Szymon Ulenberg, Krzysztof Szafrański, Tomasz Bączek

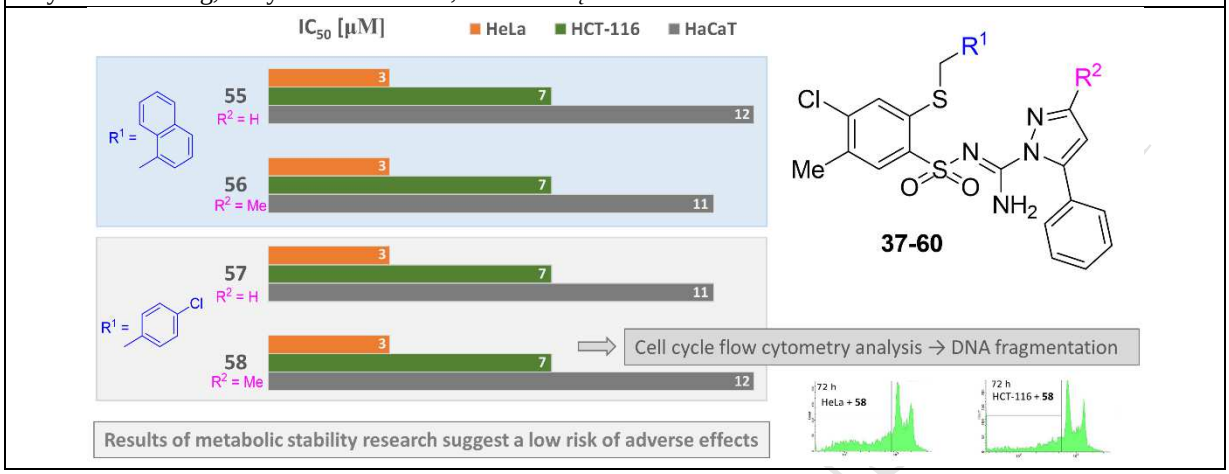

Original article

Synthesis, Molecular Structure, and Metabolic Stability of New Series of *N'*-(2-alkylthio-4-chloro-5-methylbenzenesulfonyl)-1-(5-phenyl-1*H*-pyrazol-1-yl)amidine as Potential Anti-cancer Agents

Aneta Pogorzelska [a,*], Jarosław Sławiński [a,**], Anna Kawiak [b,c], Beata Żołnowska [a], Jarosław Chojnacki [d], Grzegorz Stasiłojć[e], Szymon Ulenberg [f], Krzysztof Szafrański [a], Tomasz Bączek[f]

[a]Department of Organic Chemistry, Medical University of Gdańsk, Al. Gen. J. Hallera 107, 80-416 Gdańsk, Poland
[b]Department of Biotechnology, Intercollegiate Faculty of Biotechnology, University of Gdańsk and Medical University of Gdańsk, ul. Abrahama 58, 80-307 Gdańsk, Poland
[c]Laboratory of Human Physiology, Medical University of Gdańsk, ul. Tuwima 15, 80-210 Gdańsk, Poland
[d]Department of Inorganic Chemistry, Gdańsk University of Technology, Narutowicza 11/12, 80-233 Gdańsk, Poland
[e]Laboratory of Cell Biology, Department of Medical Biotechnology, Intercollegiate Faculty of Biotechnology UG-MUG, Medical University of Gdańsk, ul. Dębinki 1, Gdańsk 80-211, Poland
[f]Department of Pharmaceutical Chemistry, Medical University of Gdańsk, Al. Gen. J. Hallera 107, 80-416 Gdańsk, Poland

ABSTRACT

A series of new *N'*-(2-alkylthio-4-chloro-5-methylbenzenesulfonyl)-1-(5-phenyl-1*H*-pyrazol-1-yl)amidine derivatives have been synthesized and evaluated *in vitro* by MTT assays for their antiproliferative activity against cell lines of colon cancer HCT-116, cervical cancer HeLa and breast cancer MCF-7. The studied compounds display selective activity mainly against HCT-116 and HeLa cells. Thus, five compounds show selective cytotoxic effect against HCT-116 (IC_{50} = 3−10 μM) and HeLa (IC_{50} = 7 μM). Importantly, the noticed values of IC_{50} for four compounds are almost 4-fold lower for HeLa than non-malignant HaCaT cells. More-in-depth biological research revealed that the treatment of HCT-116 and HeLa with active compound resulted in increased numbers of cells in sub-G1 phase in a time dependent manner, while non-active derivative does not influence cell cycle. Metabolic stability assays using liver microsomes and NADPH provide important information on compounds susceptibility to phase 1 biotransformation reactions.

Keywords:
Benzenesulfonamides; Anticancer activity; Molecular structures; Metabolic stability; Cell cycle flow cytometry analysis

* Corresponding author.
** Corresponding author.
E-mail addresses: aneta.pogorzelska@gumed.edu.pl (A. Pogorzelska), jaroslaw@gumed.edu.pl (J. Sławiński).

1. Introduction

Neoplasms become a leading cause of morbidity and mortality worldwide which affect all of humankind. Indeed, when presented as a single entity, cancer mortality accounts 8.2 million cases and outranks deaths from every other major cause of death, as estimated in 2012. Although cancer disease affects both sexes, the faster-rising rates for women are particularly serious and worrying. Among all cancer types, cancers of breast, lung, colorectum and cervix uteri belong to the most common causes of cancer death in women [1]. Unfortunately, most anticancer drugs are still being insufficient, especially for late-stage patients, and display severe side effects. Thus, searching for new agents with cytotoxic effect toward cancer cells is one of the most important objectives of modern drug discovery.

Heterocycles play an important role in anti-cancer drug design, due to their structural and chemical diversity. These structural motifs are found in approximately two-thirds of the anticancer drugs approved by the FDA between 2010 and 2015 [2]. Among them, pyrazole ring is found in ruxolitinib, crizotinib, ibrutinib and axitinib [2], as presented in Fig. 1. Ruxolitinib is the first FDA approved therapy for the treatment of myelofibrosis and inhibits JAK1/2 [3−5]. Crizotinib acts as an ALK (anaplastic lymphoma kinase) and ROS1 (c-ros oncogene 1) inhibitor and is used in the treatment of ALK-positive non-small cell lung cancer [6−7]. Ibrutinib is approved to treat B cell cancers like mantle cell lymphoma, chronic lymphocytic leukemia, and Waldenström's macroglobulinemia, a form of non-Hodgkin's lymphoma. This drug binds permanently to Bruton's tyrosine kinase (BTK) [8−9]. Axitinib is an inhibitor of multiple receptor tyrosine kinases including vascular endothelial growth factor receptors (VEGFR-1, -2, and -3) [10]. It got approval to treat advanced renal cell carcinoma after failure of prior systemic therapy [11−13].

Aside from above-mentioned drugs, a few compounds with pyrazole ring are under clinical trials (Fig 1). Taselib (GDC 0032) is a potent and selective inhibitor of Class I PI3Kα, δ, and γ isoforms [14] which has been studied in different stages of clinical trials for breast cancer [15−22], non-small cell lung cancer [17], non-Hodgkin's lymphoma [20], solid tumors [20, 22] lymphomas [22], multiple myeloma [22], and stage IV squamous cell lung cancer [23, 24]. ODM-201 is a novel androgen receptor (AR) antagonist that blocks AR nuclear translocation [25]. It is tested under Phase 3 clinical trials for the treatment of prostate cancer [26, 27] and early Phase 1 for breast cancer [28]. A multi-CDK inhibitor for CDK1, 2, 4, 6 and 9 AT7519 (CDKI AT7519, AT7519M) [29] is studied in Phase 1 in treating patients with

solid tumors [30, 31] or refractory non-Hodgkin's lymphoma [31], or in Phase 2 in of chronic lymphocytic leukemia [32] and relapsed mantle cell lymphoma [33].

Our previous research for 2-mercaptobenzenesulfonamide derivatives (MBSA, Fig.1) revealed that compounds containing pyrazole ring display significant anticancer activity [34]. Furthermore, recent studies showed that MBSA scaffold is a valuable fragment in discovery of potential drugs against women most frequent cancers [35−40]. These results prompted us to design novel agents with the general structure of type I (Fig.1) and to study their impact on a growth of human cancer cells lines belonging to three most frequent cancers in woman: breast, colon and cervix uteri.

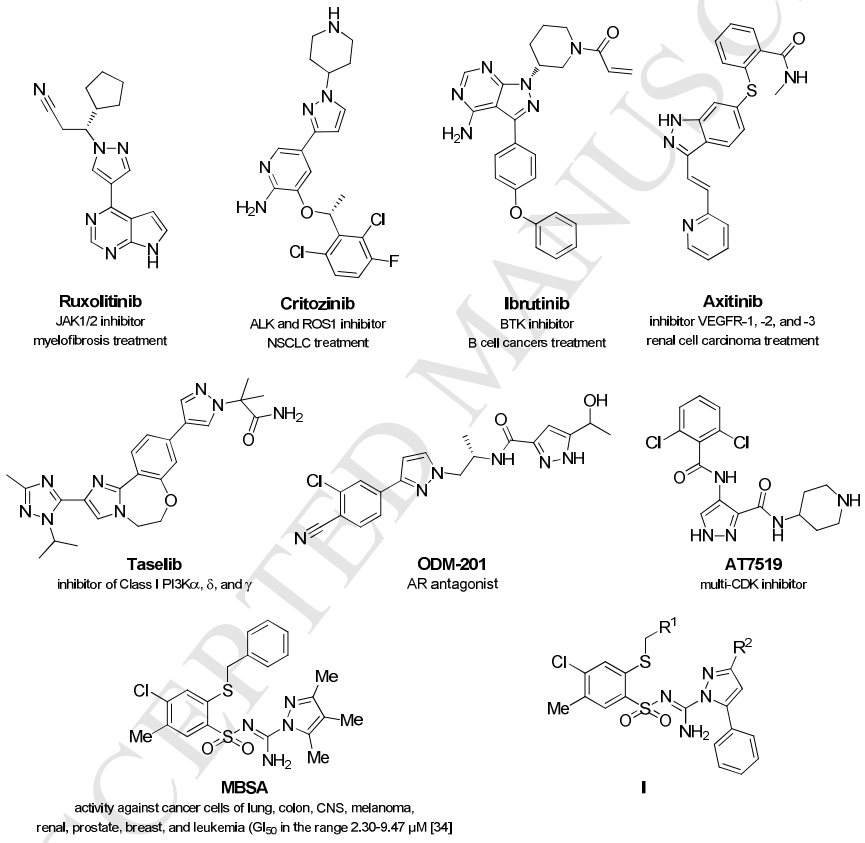

Figure 1. Selected anticancer compounds with pyrazole ring.

2. Results and discussion

2.1. Chemistry

The synthesis of novel *N'*-(2-alkylthio-4-chloro-5-methylbenzenesulfonyl)-1-(5-phenyl-1*H*-pyrazol-1-yl)amidine **37**−**60** has been presented at Scheme 1. The starting substrates, 1-amino-2-(2-alkylthio-4-chloro-5-methylbenzenesulfonyl)guanidines (**1**−**12**) and

2-(2-alkylthiobenzenesulfonyl)-3-(phenylprop-2-ynylideneamino)guanidines **13**−**36** were obtained as previously described [37,39,41,42]. The products **37**−**60** were synthesized *via* CuI-mediated electrophilic cyclizations of *α*,*β*-alkynic hydrazones, the structural fragment of compounds **13**−**36**. It should be stressed, that this step did not result with desired derivatives but led to copper complexes with pyrazole moiety. Further treatment of the obtained purple coordination complexes with 20% 4-methylbenzenesulfonic acid (PTSA) in acetonitrile gave the final compounds **37**−**60**.

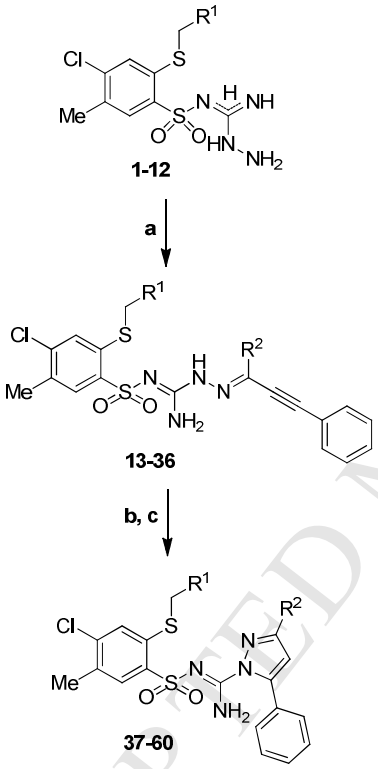

Compd	R^1	R^2
1, 13, 37	Ph	H
1, 14, 38	Ph	Me
2, 15, 39	2-MeC_6H_4	H
2, 16, 40	2-MeC_6H_4	Me
3, 17, 41	3-MeC_6H_4	H
3, 18, 42	3-MeC_6H_4	Me
4, 19, 43	4-MeC_6H_4	H
4, 20, 44	4-MeC_6H_4	Me
5, 21, 45	2-$CF_3C_6H_4$	H
5, 22, 46	2-$CF_3C_6H_4$	Me
6, 23, 47	3-$CF_3C_6H_4$	H
6, 24, 48	3-$CF_3C_6H_4$	Me
7, 25, 49	4-$CF_3C_6H_4$	H
7, 26, 50	4-$CF_3C_6H_4$	Me
8, 27, 51	2-ClC_6H_4	H
8, 28, 52	2-ClC_6H_4	Me
9, 29, 53	3-ClC_6H_4	H
9, 30, 54	3-ClC_6H_4	Me
10, 31, 55	4-ClC_6H_4	H
10, 32, 56	4-ClC_6H_4	Me
11, 33, 57		H
11, 34, 58		Me
12, 35, 59		H
12, 36, 60		Me

Scheme 1. Reagents and conditions: **a**) phenylpropiolaldehyde diethyl acetal (1 eq.) or 4-phenylbut-3-yn-2-one (1 eq.), PTSA (0.1 eq.), EtOH, reflux, 2−20 h, **b**) CuI, Et_3N, MeCN, 82 °C, 1−4 h, **c**) 20% PTSA/MeCN, 1 h.

The structures of final compounds **37**–**60** were confirmed with spectroscopic methods IR and ^{1}H NMR as well as HRMS spectrometry and elemental analyses.

The X-ray crystallography was undertaken to study both the structure of Cu-pyrazole complex and detailed tautomeric structure on representative compounds – the transition complex Cu-**46**, **57**, and **58**. The obtained molecular structures are presented in Figs. 2−4 respectively. The report and details on data collection, structure solution, refinement geometry parameters, and hydrogen bonding details for all structures are given in Supplementary Material (Appendix C and Tables 1S−5S).

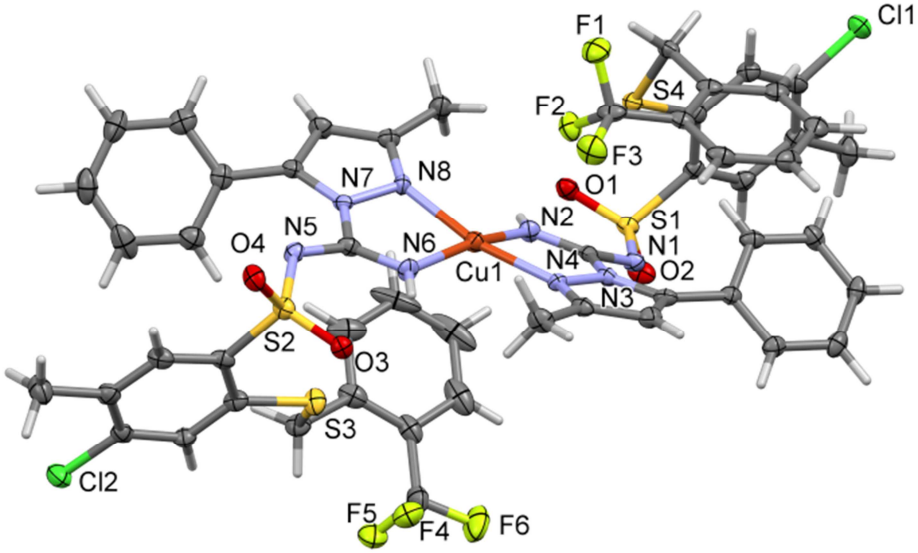

Figure 2. Molecular structure of the Cu-**46** complex, only heteroatoms are labelled, displacement ellipsoids drawn at 50% probability level. Selected bond lengths and angles (Å, °): Cu1—N2 1.901 (4), Cu1—N6 1.917 (4), Cu1—N8 1.973 (4), Cu1—N4 1.993 (4), S1—N1 1.594 (4), S2—N5 1.593(4), C1—N1 1.329(6), C1—N2 1.286(6), C1—N3 1.433(6); N2-Cu1-N6 164.54 (18), N8—Cu1—N4 167.41 (15).

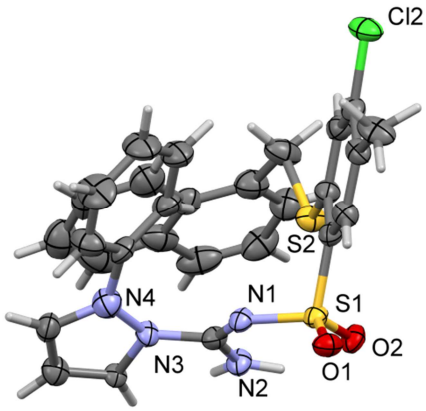

Figure 3. Molecular structure of **57**, showing heteroatom numbering scheme. Displacement ellipsoids drawn at 50% probability level.

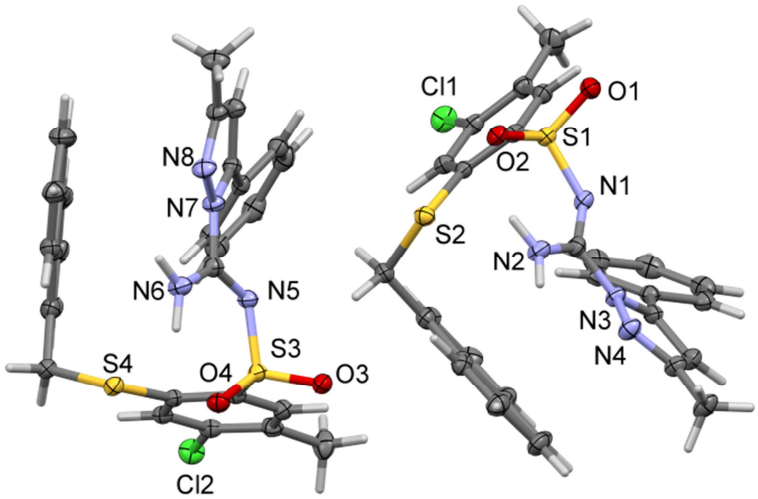

Figure 4. Molecular structure of **58**, showing heteroatom numbering scheme. Displacement ellipsoids drawn at 50% probability level. Both symmetry independent molecules shown.

2.2. Cytotoxic activity

Compounds **37**–**60** have been studied *in vitro* for their cytotoxic activity in MTT assays involving three human cancer cell lines: MCF-7 (breast cancer), HCT-116 (colon cancer) and HeLa (cervical cancer). As it was presented in Table 1, cytotoxic evaluations were expressed as IC_{50} values in μM. Among tested cell lines, HCT-116 and HeLa found to be the most susceptible to the tested derivatives while MCF-7 displayed slightly reduced susceptibility.

Table 1. IC_{50} values for compounds **37**-**60**

Compd	R^1	R^2	IC_{50} [μM]			
			HCT-116	HeLa	MCF-7	HaCaT
37	Ph	H	12±0.5	5±0,1	20±1	18±1
38	Ph	Me	10±0.5	5±0,1	15±0,3	10±0.1
39	2-MeC_6H_4	H	16±0,3	17±0,5	23±0,5	18±0.2
40	2-MeC_6H_4	Me	42±1	160±3	80±2	-
41	3-MeC_6H_4	H	6.5±0,1	8±0,5	47±1	10±0.1
42	3-MeC_6H_4	Me	34±1	155±5	105±5	-
43	4-MeC_6H_4	H	14±1	17±1	21±1	20±0.5
44	4-MeC_6H_4	Me	28±1	62±2	89±4	30±1
45	2-$CF_3C_6H_4$	H	16±0,5	20±0,3	21±0,2	20±0.2
46	2-$CF_3C_6H_4$	Me	25±0,5	215±4	101±3	-
47	3-$CF_3C_6H_4$	H	14±0.1	19±0.5	17±0.5	18±1
48	3-$CF_3C_6H_4$	Me	19±0.2	98±1	41±2	40±1
49	4-$CF_3C_6H_4$	H	14±0.3	17±1	25±1	19±1
50	4-$CF_3C_6H_4$	Me	7±0.1	19±0.5	16±0.2	18±1
51	2-ClC_6H_4	H	18±1	19±0,2	24±0,3	20±0.2
52	2-ClC_6H_4	Me	170±3	270±16	135±7	-

53	3-ClC_6H_4	H	7±0,1	10±0,3	88±2	10±0.3
54	3-ClC_6H_4	Me	18±0,2	8±0,5	25±1	18±1
55	4-ClC_6H_4	H	7±0.1	3±0.03	75±1	12±0.2
56	4-ClC_6H_4	Me	7±0.1	3±0.03	108±1	11±0.2
57	1-naphthyl	H	7±0.03	3±0.03	58±1	11±0.1
58	1-naphthyl	Me	7±0.1	3±0.03	170±3	12±0.1
59	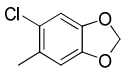	H	32±0.3	160±5	105±4	105±4
60	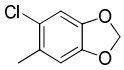	Me	100±3	180±5	145±7	-
Cisplatin			3.8 ± 0.2	2.2 ± 0.1	3.0 ± 0.1	

Regarding cytotoxicity against HCT-116, high activity was noticed for 7 compounds (**41**, **50**, **53** and **55**−**58**) with IC_{50} around 7 μM. Slightly weaker growth inhibition, with 7 μM < IC_{50} < 20 μM, was observed for derivatives **37**−**39**, **43**, **45**, **47**−**49**, **51** and **54**. The remaining compounds, with the exception of inactive **52** and **60**, displayed moderate cytotoxicity with IC_{50} values in the range of 25−42 μM.

The strongest inhibition of growth of HeLa cell line was observed for compounds **55**−**58** (IC_{50} = 3 μM), although five other derivatives (**37**−**38**, **41** and **53**−**54**) displayed good activity with $IC_{50} \leq 10$ μM. Moderate cytotoxic effects, with IC_{50} around 20 μM, were found for compounds **39**, **43**, **45**, **47** and **49**−**51**. The remaining derivatives were found to be inactive against HeLa cells.

A slightly weaker activity was observed against MCF-7 cells. The noticeable IC_{50} value around 16 μM was noticed for compounds **38**, **47** and **50**. The moderate cytotoxic effect, defined by IC_{50} in the range of 20−47 μM, was found for derivatives **38**, **39**, **41**, **43**, **45**, **48**, **49**, **51** and **54**. The other compounds did not inhibit the growth of MCF-7 cells significantly.

Based on the results of MTT assays, the activity of a new series of derivatives is dependent on the relation between the structures of R^1 and R^2 groups. In general, compounds **37**−**38** with R^1 = Ph displayed significant inhibition of the growth of all tested cell lines, regardless of R^2 group. In turn, the activity of compounds **39**−**41**, substituted with methyl in benzene ring of R^1, was strongly related to R^2 type. It was noticed that derivatives with R^2 = H were significantly more potent compared to those with R^2 = Me. It is also worthwhile to mention that in this series, compound **41** (R^1 = 3-MeC_6H_4, R^2 = H) displayed remarkable selectivity towards HCT-116 and HeLa cells, with IC_{50} = 8 μM and IC_{50} = 6.5 μM, respectively (IC_{50} = 47 μM for MCF-7). The quite similar R^1-R^2 relationships were observed for compounds **45**−**48** containing trifluoromethyl at *ortho* and *meta* position in R^1 structure.

However, the relation between R^1 and R^2 structures was not significant for the activity of compounds **47**−**48** against HCT-116.

In series **51**−**58** with chlorine atom as substituent in R^1, only derivatives **51**−**52** with R^1 = 2-ClC_6H_4 displayed a similar R^2-related activity. Compound **51** (R^2 = H) inhibited the growth of all tested cell lines while **52** was inactive. In turn, the R^2 alteration for compounds **53** and **54** (R^1 = 3-ClC_6H_4) resulted in similar activity against HeLa line (IC_{50} = 10 μM and 8 μM for **53** and **54**, respectively). Interestingly, substitution with R^2 = Me in **54** led to increased growth inhibition of MCF-7 cells (IC_{50} = 88 μM and 25 μM for **53** and **54**, respectively). Regarding the incorporation of chlorine atom at *para* position in R^1 structure, either compound **55** or **56** greatly affected the growth of HCT-116 and HeLa cells, with IC_{50} for both **55** and **56** at the level of 7 μM and 3 μM against HCT-116 and HeLa, correspondingly. The same results were noticed for compounds **57**−**58** with R^1 = 1-naphthyl. Importantly, neither of compounds **55**−**58** was active against MCF-7 cells.

Analysis of the obtained results indicated that there is interesting R^2-dependent selectivity against HCT-116. The data for compounds **39**−**56** showed that an incorporation of methyl or trifluoromethyl in R^1 and R^2 = Me led to noticeable selectivity toward HCT-116 (see compd **40**, **42**, **44**, **46**, **48** and **50** in Table 1; on average, IC_{50} values for HCT-116 were 2.2−8.6-fold higher than both HeLa and MCF-7). This trend was not observed for compounds with chlorine atom in R^1 structure, whatever R^2 type (compd **51**−**56**). A slightly different observation was noticed for compounds **59**−**60**, modified by R^1 = 6-chlorobenzo[*d*]1,3-dioxol-5-yl moiety. In contrast to most derivatives, inhibition of HCT-116 cells growth, with IC_{50} = 32 μM, was observed for **59** which contains R^2 = H; neither HeLa nor MCF-7 cells display important sensitivity. Derivative **60**, in turn, did not affect the cells growth of tested lines.

For the compounds with the strongest cytotoxicity as well as derivatives with selective activity, an investigation of cytotoxic effect against non-carcinogenic cell line HaCaT was done. Promising selectivity toward HeLa cells have been observed for six derivatives **37** and **54**−**58** (Table 1, Figure 5). The activity against HeLa cells was at least 2.25-fold (**54**) higher when compared with HaCaT cell line. The best selectivity has been noticed for compounds **55**−**58** with almost 4-fold lower IC_{50} against HeLa than observed in HaCaT cells (Table 1, Figure 5). The inhibition of HCT-116 growth with a low impact on HaCaT growing was observed for compounds **50** and **59**. The IC_{50} values were 2.6 or 3.28-fold lower for HCT-116 than for HaCaT cells for **50** and **59**, respectively.

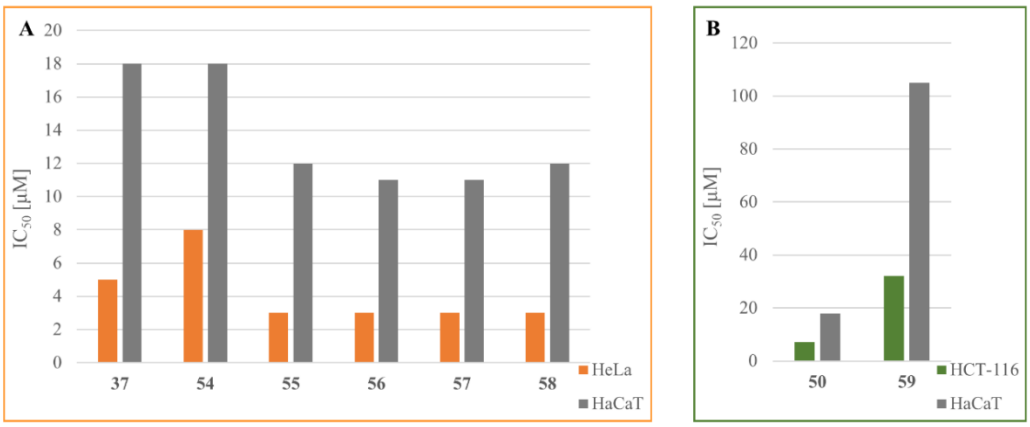

Figure 5. Selectivity of compd **A**) **37** and **54-58** against HeLa, and **B**) **50**, **59** against HCT-116 as compared to HaCaT cells.

2.3. Cell Cycle Analysis

To assess whether new derivatives influence the cell cycle, HCT-116 and HeLa cells were treated with 50 μM **58** for 24 h, 48 h, and 72 h (Figure 6). In order to check if non-active compounds have any impact on the cell cycle, the experiment with **60** was made at the same conditions.

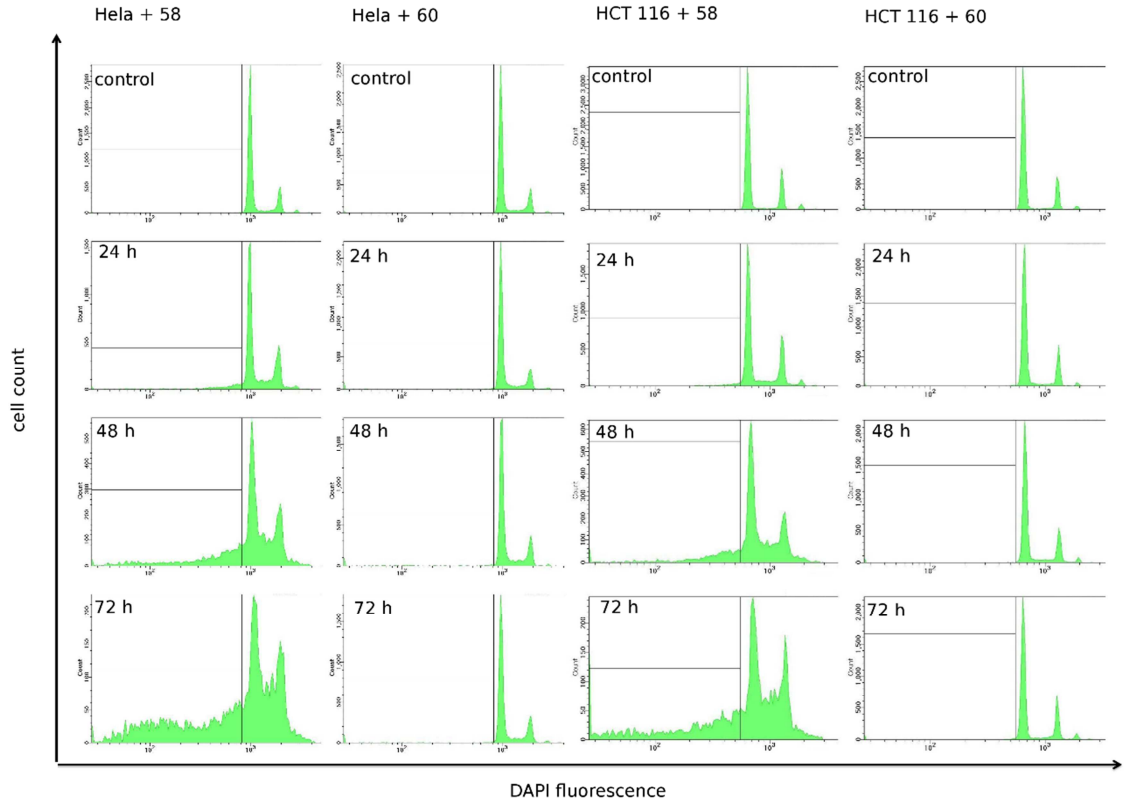

Figure 6. HCT-116 and HeLa cell cycle induction with **58** and **60** after 24 h, 48 h, and 72 h.

The results of this analysis (Figure 7) show the significant increase in the cell distribution in the sub-G1 phase in a time-dependent manner in the **58**-treated group (HCT-116 from 3.86 ± 2.32% (control) to 42.99% ± 11.82%; HeLa from 7.49 ± 3.43% (control) to 51.4% ± 8.58%), by contrast with control or **60**-treated group.

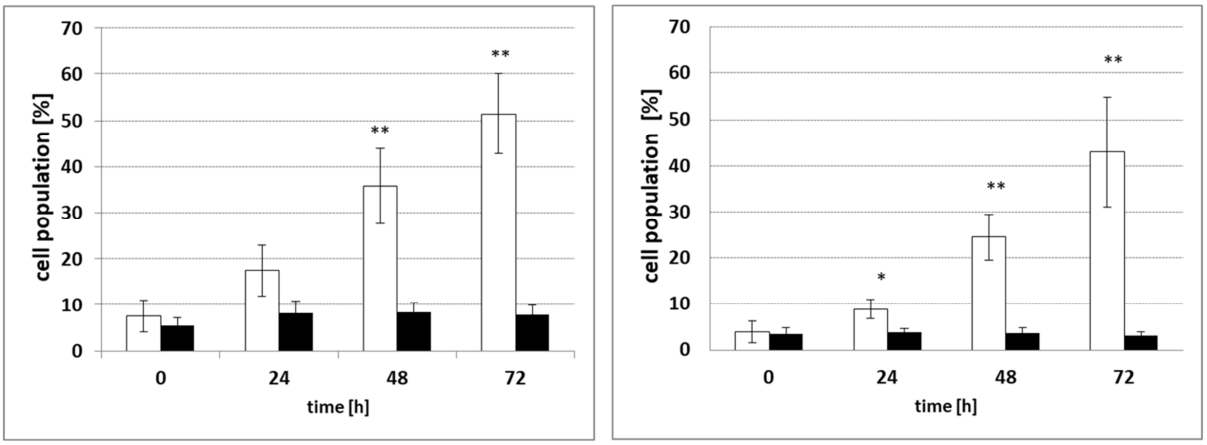

Figure 7. Sub-G1 phase of cell cycle in HeLa and HCT-116 after treatment with compounds **58** (white bars) and **60** (black bars). Cells were incubated with compounds for 24 – 72 h, respectively. Cell populations data are expressed as the mean ± SD of at least three independent experiments. * $p<0.05$; ** $p<0.01$

As it is shown on Figure 5, the impact of **58** and **60** on HeLa and HCT-116 cells differ in terms of DNA fragmentation. Between cells treated with compound **58** and compound **60** one can clearly see that the number of sub-G1 cells population is measurably high.

2.4. Metabolic stability

The results of compound incubations in the presence of pooled human liver microsomes and NADPH are presented in Table 2. Metabolic stability is presented in form of a microsomal half-life value, which enables easy comparison of compounds structures and their susceptibility to phase 1 biotransformation reactions (which is a result of incubation in the presence of human liver microsomes and NADPH).

Table 2. Experimental $t_{1/2}$ values along with corresponding SD.

Compd	**R^1**	**R^2**	**Average $t_{1/2}$ [min](n=2)**	**SD [min]**
37	Ph	H	4.63	1.10
38	Ph	Me	5.63	0.06

39	2-MeC_6H_4	H	4.81	0.52
40	2-MeC_6H_4	Me	9.23	2.93
41	3-MeC_6H_4	H	13.89	2.18
42	3-MeC_6H_4	Me	12.82	3.55
43	4-MeC_6H_4	H	7.80	4.26
44	4-MeC_6H_4	Me	10.57	2.39
45	2-$CF_3C_6H_4$	H	9.02	0.76
46	2-$CF_3C_6H_4$	Me	18.38	0.93
47	3-$CF_3C_6H_4$	H	5.18	0,27
48	3-$CF_3C_6H_4$	Me	10.13	0.26
49	4-$CF_3C_6H_4$	H	10.57	2.39
50	4-$CF_3C_6H_4$	Me	14.43	1.32
51	2-ClC_6H_4	H	13.53	0.91
52	2-ClC_6H_4	Me	9.75	0.64
53	3-ClC_6H_4	H	18.54	0.42
54	3-ClC_6H_4	Me	12.27	2.02
55	4-ClC_6H_4	H	20.37	1.73
56	4-ClC_6H_4	Me	14.41	0.25
57	1-naphthyl	H	16.09	1.03
58	1-naphthyl	Me	15.36	2.01
59	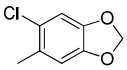	H	14.44	2.11
60	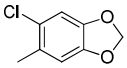	Me	11.86	0.38

SD – standard deviation

Studied compounds represent a very diverse group when it comes to metabolic stability analysis. Microsomal half-life values range from less than 5 minutes to 20 minutes. That allows to perform a visual analysis of relationships between structure of studied compounds and their metabolic stability. Metabolic stability of compounds with R^1 = Ph (**37**, **38**), 2-MeC_6H_4 (**39**, **40**), 4-MeC_6H_4 (**43**, **44**), 2-$CF_3C_6H_4$ (**45**, **46**), 3-$CF_3C_6H_4$ (**47**, **48**), and 4-CF_3C_6H (**49**, **50**) moieties enhances with methyl group in R^2 position. Such conclusion, due to high standard deviation, can also be assumed about derivatives with R^1 = 3-MeC_6H_4 moiety (**41**, **42**), even though mean half-time says otherwise. For other compounds the methyl group in R^2 position actually decreased metabolic stability. The least stable compound possesses R^1 = Ph group, smallest of all presented moieties. Hence, it can be assumed that size of moiety in R^1 position has an impact on metabolic stability (the bigger the moiety, the higher the metabolic stability).

Among studied derivatives, the most stable is **55** ($t_{1/2}$ = 20.37 min) (R^1 = 4-ClC_6H_4, R^2 = H), and the most susceptible to biotransformation is **37** ($t_{1/2}$ = 4.63 min) (R^1 = Ph, R^2 = H). Compounds with highest stability (**55**−**58**) can be characterized by higher metabolic stability values ($t_{1/2}$ > 15 min), but also a very good activity towards HeLa and HCT-116 cell lines. Compounds **41**, **49**−**51**, **54**, and **56** represent a group with semi-high metabolic stability values ($t_{1/2}$ = 10−15 min). From this group, compounds **49**−**51** and **54** are active towards all three tested cell lines, which, compared with their metabolic stability values makes them worthy candidates for further studies. Compounds **37**−**39**, **43**, **45**, and **47** are very active towards all 3 cancer cell lines, yet their metabolic stability values are the smallest of all studied set of compounds ($t_{1/2}$ < 10 min). Considering the fact, that compounds with high metabolic stability can often cause adverse drug reactions (the longer the drug stays unchanged by biotransformation in organism, the bigger such chance), compounds from the semi-stable group are not only active, but might also be the safest to use when considering adverse drug reactions occurrence chance.

3. Conclusions

We have developed methods for the preparation of novel series of *N'*-(2-alkylthio-4-chloro-5-methylbenzenesulfonyl)-1-(5-phenyl-1*H*-pyrazol-1-yl)amidine derivatives. The crystallographic analysis revealed that during pyrazole synthesis *via* CuI-mediated electrophilic cyclizations the final compounds are in the anionic form, deprotonated at NH_2 groups, and create a “salt like” complex with copper atom.

The obtained compounds were evaluated *in vitro* by MTT assay for their antiproliferative activity against three cancer cell lines: colon HCT-116, cervical HeLa and breast MCF-7. We have found that novel derivatives are strong growth inhibitors of HCT-116 and HeLa. Especially, the strongest effects were observed for compounds **55**−**56** (R^1 = 4-ClC_6H_4) and **57**−**58** (R^1 = 1-naphthyl) with IC_{50} values 7 μM and 3 μM, against HCT-116 and HeLa, respectively. What important, the observed HeLa growth inhibition for compounds **55**−**58** was almost 4-fold stronger than observed for non-carcinogenic HaCaT. Furthermore, rather short metabolic stability of novel compounds makes them good candidates for further studies considering adverse drug reactions occurrence chance.

Structure-activity relationship indicated that selective cytotoxic effect against cancer cell lines depend on a kind and place of group in R^1 residue with different R^2-dependency. For compounds with R^2 = Me, the bulky groups placed at *ortho* or *meta* in R^1 of **40** (R^1 = 2-MeC_6H_4), **42,** (R^1 = 3-MeC_6H_4), **46** (R^1 = 2-$CF_3C_6H_4$), and **48** (R^1 = 3-$CF_3C_6H_4$) resulted in

significant selectivity against HCT-116 cells. Incorporation of R^1 = 2-ClC_6H_4 in compound **52**, in turn, led to no inhibitory effect on the growth of tested cell lines, while substitution by R^1 = 3-ClC_6H_4 in **54** resulted in a high activity against HeLa cells and a slightly lower cytotoxicity against HCT-116 and MCF-7 cells. The activity of *para*-substituted compounds is related to a steric and electronic effect of groups in R^1. The bulky and high-electronegative trifluoromethyl group (**49**−**50**) is responsible for high overall cytotoxicity, methyl moiety (R^2) (**43**−**44**) results in a slight decrease in cytotoxicity as well as R^2-dependent selectivity, and chlorine atom (**55**−**56**) leads to great and selective inhibition of HCT-116 and HeLa cells growth.

The treatment of HCT-116 and HeLa with compound **58** resulted in increased numbers of cells in sub-G1 phase, as was shown by DNA flow cytometric analysis. Prolongation of incubation time for 24 h, 48 h, and 72 h resulted in a significant increase in DNA damage.

4. Experimental protocols

4.1. Synthesis

Melting points were determined with a Boethius apparatus. Infrared (IR) spectroscopy was carried out on Thermo Mattson Satellite FTIR spectrophotometer. ^{1}H and ^{13}C nuclear magnetic resonance (NMR) spectra were recorded on Varian Gemini 200 apparatus at 200 MHz (^{1}H NMR) or on a Varian Unity 500 Plus apparatus at 500 MHz (^{1}H NMR) and 125 MHz (^{13}C NMR). The chemical shifts are expressed in parts per million (ppm) relative to TMS as an internal standard. The elemental analyses were performed using PerkinElmer 2400 Series II CHN Elemental Analyzer. The results for C, H and N were in agreement with the theoretical values within ±0.4% range.

Commercially unavailable substrates were obtained according to the following methods described previously: 1-amino-2-(2-alkylthio-4-chloro-5-methylbenzenesulfonyl)guanidine derivatives **1** [41] **2**, **3**, **5**, and **8-9** [37], **4**, **6**, **7**, **10**, **12** [42], and **11** [39], and 2-(2-alkylthiobenzenesulfonyl)-3-(phenylprop-2-ynylideneamino)guanidine derivatives **13-36** [37].

*4.1.1. Procedures for the preparation of N'-(2-alkylthio-4-chloro-5-methylbenzenesulfonyl)-1-(5-phenyl-1H-pyrazol-1-yl)amidine **37-60***

To a stirred suspension of the appropriate 2-(2-alkylthiobenzenesulfonyl)-3-(3-phenylprop-2-ynylideneamino)guanidine (**13**-**36**) (0.5 mmol) in acetonitrile (4 mL) under argon atmosphere, CuI (0.25 mmol, 0.095 g) and Et_3N (0.4 mmol, 0.056 mL) were added. The resulting mixture was stirred at 82 °C for 1−4 h and the obtained purple precipitate was filtered off, dried and treated by 3 mL of 20% PTSA solution in MeCN. After stirring for 1 h, the solvent was evaporated, and 5 mL of water was added to the residue. The obtained white precipitate was filtered off, and, after drying, crystallized from the appropriate solvent to afford the desired pure product.

*4.1.1.1. N'-(2-Benzylthio-4-chloro-5-methylbenzenesulfonyl)-1-(5-phenyl-1H-pyrazol-1-yl)amidine (**37**)*

Starting from **13** (0.249 g) with stirring for 4 h, the title compound **37** was obtained after crystallization from MeCN (0.107 g, 43%): m.p. 112−115 °C; IR (KBr): 3397, 3226 (NH), 1645 (NH), 1560, 1543, 1494, 1436 (C=C, C=N), 1300, 1139 (SO_2) cm^{-1}; ^1H NMR (200 MHz, DMSO-d_6): δ 2.27 (s, 3H, CH_3), 4.24 (s, 2H, SCH_2), 6.88 (d, J = 1.5 Hz, 1H, H-4 pyrazole), 6.81−7.08 (m, 5H, arom.), 7.18−7.33 (m, 5H, arom.), 7.46 (s, 1H, H-3), 7.49 (s, 1H, H-6), 7.92 (d, J = 1.5 Hz, 1H, H-3 pyrazole), 8.17 (s, 1H, NH), 9.15 (s, 1H, NH) ppm; HRMS (ESI-TOF) *m/z* calcd for $C_{24}H_{21}ClN_4O_2S_2$ [M+H^+] 497.0867, found 497.0592. Anal. ($C_{24}H_{21}ClN_4O_2S_2$) C, H, N.

*4.1.1.2. N'-(2-Benzylthio-4-chloro-5-methylbenzenesulfonyl)-1-(3-methyl-5-phenyl-1H-pyrazol-1-yl)amidine (**38**)*

Starting from **14** (0.255 g) with stirring for 1 h, the title compound **38** was obtained after crystallization from *i*-PrOH (0.094 g, 37%): m.p. 123−126 °C; IR (KBr): 3445, 3331 (NH), 1637 (NH), 1527, 1449, 1423 (C=C, C=N), 1289, 1132 (SO_2) cm^{-1}; ^1H NMR (200 MHz, DMSO-d_6): δ 2.22 (s, 3H, CH_3), 2.27 (s, 3H, CH_3), 4.25 (s, 2H, SCH_2), 6.39 (s, 1H, H-4 pyrazole), 6.77−7.05 (m, 5H, arom.), 7.19−7.29 (m, 5H, arom.), 7.43 (s, 1H, H-3), 7.50 (s, 1H, H-6), 8.01 (s, 1H, NH), 8.94 (s, 1H, NH) ppm; HRMS (ESI-TOF) *m/z* calcd for $C_{25}H_{23}ClN_4O_2S_2$ [M+H^+] 511.1024, found 511.1017. Anal. ($C_{25}H_{23}ClN_4O_2S_2$) C, H, N.

*4.1.1.3. N'-{4-Chloro-5-methyl-2-[(2-methylphenyl)methylthio]benzenesulfonyl}-1-(5-phenyl-1H-pyrazol-1-yl)amidine (**39**)*

Starting from **15** (0.255 g) with stirring for 2 h, the title compound **39** was obtained after crystallization from MeCN (0.199 g, 78%): m.p. 134−137 °C; IR (KBr): 3420, 3316 (NH),

1656 (NH), 1539, 1494, 1462, 1425 (C=C, C=N), 1288, 1132 (SO_2) cm^{-1}; ^1H NMR (500 MHz, DMSO-d_6): δ 2.23 (s, 3H, CH_3), 2.30 (s, 3H, CH_3), 4.23 (s, 2H, SCH_2), 6.57 (s, 1H, H-4 pyrazole), 6.86 (t, 2H, arom.), 6.99−7.13 (m, 6H, arom.), 7.25 (d, *J* = 6.9 Hz, 1H, arom.), 7.48 (s, 1H, H-3), 7.55 (s, 1H, H-6), 7.91 (s, 1H, H-3 pyrazole), 8.10 (s, 1H, NH), 9.09 (s, 1H, NH) ppm; ; HRMS (ESI-TOF) *m/z* calcd for $C_{25}H_{23}ClN_4O_2S_2$ [M+H^+] 511.1024, found 511.1027. Anal. ($C_{25}H_{23}ClN_4O_2S_2$) C, H, N.

*4.1.1.4. N'-{4-Chloro-5-methyl-2-[(2-methylphenyl)methylthio]benzenesulfonyl}-1-(3-methyl-5-phenyl-1H-pyrazol-1-yl)amidine (**40**)*

Starting from **16** (0.262 g) with stirring for 2 h, the title compound **40** was obtained after crystallization from EtOH (0.118 g, 45%): m.p. 154−156 °C; IR (KBr): 3460, 3343 (NH), 1638 (NH), 1530, 1446, 1425 (C=C, C=N), 1291, 1135 (SO_2) cm^{-1}; ^1H NMR (500 MHz, DMSO-d_6): δ 2.24 (s, 3H, CH_3), 2.29 (s, 3H, CH_3), 2.30 (s, 3H, CH_3), 4.24 (s, 2H, SCH_2), 6.40 (s, 1H, H-4 pyrazole), 6.83 (t, 2H, arom.), 6.97 (d, *J* = 7.3 Hz, 2H, arom.), 7.02 (t, 1H, arom.), 7.07−7.15 (m, 3H, arom.), 7.25 (d, *J* = 7.4 Hz, 1H, arom.), 7.45 (s, 1H, H-3), 7.56 (s, 1H, H-6), 7.94 (s, 1H, NH), 8.89 (s, 1H, NH) ppm; HRMS (ESI-TOF) *m/z* calcd for $C_{26}H_{25}ClN_4O_2S_2$ [M+H^+] 525.1180, found 525.1182. Anal. ($C_{26}H_{25}ClN_4O_2S_2$) C, H, N.

*4.1.1.5. N'-{4-Chloro-5-methyl-2-[(3-methylphenyl)methylthio]benzenesulfonyl}-1-(5-phenyl-1H-pyrazol-1-yl)amidine (**41**)*

Starting from **17** (0.255 g) with stirring for 3 h, the title compound **41** was obtained after crystallization from MeCN (0.145 g, 57%): m.p. 119−122 °C; IR (KBr): 3425, 3321 (NH), 1650 (NH), 1535, 1498, 1463, 1427 (C=C, C=N), 1294, 1131 (SO_2) cm^{-1}; ^1H NMR (500 MHz, DMSO-d_6): δ 2.17 (s, 3H, CH_3), 2.28 (s, 3H, CH_3), 4.20 (s, 2H, SCH_2), 6.59 (s, 1H, H-4 pyrazole), 6.83 (t, 2H, arom.), 6.95−7.05 (m, 4H, arom.), 7.09−7.11 (m, 3H, arom.), 7.45 (s, 1H, H-3), 7.50 (s, 1H, H-6), 7.92 (s, 1H, H-3 pyrazole), 8.16 (s, 1H, NH), 9.15 (s, 1H, NH) ppm; HRMS (ESI-TOF) *m/z* calcd for $C_{25}H_{23}ClN_4O_2S_2$ [M+H^+] 511.1024, found 511.1025. Anal. ($C_{25}H_{23}ClN_4O_2S_2$) C, H, N.

*4.1.1.6. N'-{4-Chloro-5-methyl-2-[(3-methylphenyl)methylthio]benzenesulfonyl}-1-(3-methyl-5-phenyl-1H-pyrazol-1-yl)amidine (**42**)*

Starting from **18** (0.262 g) with stirring for 1 h, the title compound **42** was obtained after crystallization from MeCN (0.118 g, 45%): m.p. 152−156 °C; IR (KBr): 3392 (NH), 1656 (NH), 1566, 1534, 1461, 1430 (C=C, C=N), 1291, 1139 (SO_2) cm^{-1}; ^1H NMR (500 MHz,

DMSO-d_6): δ 2.24 (s, 3H, CH_3), 2.29 (s, 3H, CH_3), 2.30 (s, 3H, CH_3), 4.24 (s, 2H, SCH_2), 6.40 (s, 1H, H-4 pyrazole), 6.83 (t, 2H, arom.), 6.97 (d, *J* = 7.3 Hz, 2H, arom.), 7.02 (t, 1H, arom.), 7.07−7.15 (m, 3H, arom.), 7.25 (d, *J* = 6.9 Hz, 1H, arom.), 7.45 (s, 1H, H-3), 7.56 (s, 1H, H-6), 7.94 (s, 1H, NH), 8.89 (s, 1H, NH) ppm; HRMS (ESI-TOF) *m/z* calcd for $C_{26}H_{25}ClN_4O_2S_2$ [M+H^+] 525.1180, found 525.1178. Anal. ($C_{26}H_{25}ClN_4O_2S_2$) C, H, N.

*4.1.1.7. N'-{4-Chloro-5-methyl-2-[(4-methylphenyl)methylthio]benzenesulfonyl}-1-(5-phenyl-1H-pyrazol-1-yl)amidine (**43**)*

Starting from **19** (0.255 g) with stirring for 2 h, the title compound **43** was obtained after crystallization from EtOH (0.067 g, 25%): m.p. 128−131 °C; IR (KBr): 3425, 3321 (NH), 1650 (NH), 1535, 1498, 1463, 1427 (C=C, C=N), 1294, 1131 (SO_2) cm^{-1}; ^{1}H NMR (200 MHz, DMSO-d_6): δ 2.18 (s, 3H, CH_3), 2.28 (s, 3H, CH_3), 4.21 (s, 2H, SCH_2), 6.59 (d, *J* = 0.6 Hz, 1H, H-4 pyrazole), 6.82−7.09 (m, 7H, arom.), 7.19 (d, *J* = 7.9 Hz, 2H, arom.), 7.45 (s, 1H, H-3), 7.51 (s, 1H, H-6), 7.93 (d, *J* = 0.6 Hz ,1H, H-3 pyrazole), 8.16 (s, 1H, NH), 9.15 (s, 1H, NH) ppm; HRMS (ESI-TOF) *m/z* calcd for $C_{25}H_{23}ClN_4O_2S_2$ [M+H^+] 511.1024, found 511.1002. Anal. ($C_{25}H_{23}ClN_4O_2S_2$) C, H, N.

*4.1.1.8. N'-{4-Chloro-5-methyl-2-[(4-methylphenyl)methylthio]benzenesulfonyl}-1-(3-methyl-5-phenyl-1H-pyrazol-1-yl)amidine (**44**)*

Starting from **20** (0.262 g) with stirring for 2.5 h, the title compound **44** was obtained after crystallization from MeCN (0.157 g, 60%): m.p. 156−159 °C; IR (KBr): 3464, 3345 (NH), 1636 (NH), 1526, 1449 (C=C, C=N), 1285, 1128 (SO_2) cm^{-1}; ^{1}H NMR (200 MHz, DMSO-d_6): δ 2.19 (s, 3H, CH_3), 2.28 (s, 3H, CH_3), 2.31 (s, 3H, CH_3), 4.22 (s, 2H, SCH_2), 6.42 (s, 1H, H-4 pyrazole), 6.79−7.02 (m, 7H, arom.), 7.19 (d, *J* = 7.9 Hz, 2H, arom.), 7.42 (s, 1H, H-3), 7.52 (s, 1H, H-6), 7.99 (s, 1H, NH), 8.93 (s, 1H, NH) ppm; HRMS (ESI-TOF) *m/z* calcd for $C_{26}H_{25}ClN_4O_2S_2$ [M+H^+] 525.1180, found 525.1166. Anal. ($C_{26}H_{25}ClN_4O_2S_2$) C, H, N.

*4.1.1.9. N'-{4-Chloro-5-methyl-2-[(2-trifluoromethylphenyl)methylthio]benzenesulfonyl}-1-(5-phenyl-1H-pyrazol-1-yl)amidine (**45**)*

Starting from **21** (0.283 g) with stirring for 3 h, the title compound **45** was obtained after crystallization from EtOH (0.082 g, 29%): m.p. 114−116 °C; IR (KBr): 3432, 3350 (NH), 1651 (NH), 1530, 1506, 1447, 1422 (C=C, C=N), 1321, 1135 (SO_2) cm^{-1}; ^{1}H NMR (500 MHz, DMSO-d_6): δ 2.27 (s, 3H, CH_3), 4.32 (s, 2H, SCH_2), 6.42 (s, 1H, H-4 pyrazole), 6.87 (t, 2H, arom.), 7.02−7.06 (m, 3H, arom.), 7.40 (s, 1H, H-3), 7.47−7.50 (m, 2H, H-6, arom.),

7.55 (m, 2H, arom.), 7.70 (d, *J* = 7.4 Hz, 1H, arom.), 7.91 (s, 1H, H-3 pyrazole), 8.01 (s, 1H, NH), 8.90 (s, 1H, NH) ppm; HRMS (ESI-TOF) *m/z* calcd for $C_{25}H_{20}ClF_3N_4O_2S_2$ [M+H$^+$] 565.0741, found 565.0737. Anal. ($C_{25}H_{20}F_3ClN_4O_2S_2$) C, H, N.

*4.1.1.10. N'-{4-Chloro-5-methyl-2-[(2-trifluoromethylphenyl)methylthio]benzenesulfonyl}-1-(3-methyl-5-phenyl-1H-pyrazol-1-yl)amidine (**46**)*

Starting from **22** (0.290 g) with stirring for 1.5 h, the title compound **46** was obtained after crystallization from MeCN (0.115 g, 40%): m.p. 130−133 °C; IR (KBr): 3466, 3354 (NH), 1652 (NH), 1583, 1569, 1528, 1446 (C=C, C=N), 1319, 1134 (SO_2) cm^{-1}; ^{1}H NMR (500 MHz, DMSO-d_6): δ 2.28 (s, 3H, CH_3), 2.29 (s, 3H, CH_3), 4.35 (s, 2H, SCH_2), 6.41 (s, 1H, H-4 pyrazole), 6.88 (t, 2H, arom.), 7.01−7.05 (m, 3H, arom.), 7.41 (s, 1H, H-3), 7.46−7.49 (m, 2H, H-6, arom.), 7.56 (m, 2H, arom.), 7.70 (d, *J* = 7.3 Hz, 1H, arom), 7.98 (s, 1H, NH), 8.90 (s, 1H, NH) ppm; HRMS (ESI-TOF) *m/z* calcd for $C_{26}H_{22}ClF_3N_4O_2S_2$ [M+H$^+$] 579.0898, found 579.0892. Anal. ($C_{26}H_{22}F_3ClN_4O_2S_2$) C, H, N.

*4.1.1.11. N'-{4-Chloro-5-methyl-2-[(3-trifluoromethylphenyl)methylthio]benzenesulfonyl}-1-(5-phenyl-1H-pyrazol-1-yl)amidine (**47**)*

Starting from **23** (0.283 g) with stirring for 1 h, the title compound **47** was obtained after crystallization from MeCN (0.088 g, 31%): m.p. 121−124 °C; IR (KBr): 3432, 3404 (NH), 1655 (NH), 1532, 1464, 1446, 1427 (C=C, C=N), 1330, 1126 (SO_2) cm^{-1}; ^{1}H NMR (200 MHz, DMSO-d_6): δ 2.29 (s, 3H, CH_3), 4.40 (s, 2H, SCH_2), 6.60 (d, *J* = 1.7 Hz, 1H, H-4 pyrazole), 6.79−7.06 (m, 5H, arom.), 7.40−7.73 (m, 6H, arom.), 7.94 (d, *J* = 1.6 Hz, 1H, H-3 pyrazole), 8.22 (s, 1H, NH), 9.19 (s, 1H, NH) ppm; HRMS (ESI-TOF) *m/z* calcd for $C_{25}H_{20}ClF_3N_4O_2S_2$ [M+H$^+$] 565.0741, found 565.0737. Anal. ($C_{25}H_{20}F_3ClN_4O_2S_2$) C, H, N.

*4.1.1.12. N'-{4-Chloro-5-methyl-2-[(3-trifluoromethylphenyl)methylthio]benzenesulfonyl}-1-(3-methyl-5-phenyl-1H-pyrazol-1-yl)amidine (**48**)*

Starting from **24** (0.290 g) with stirring for 2 h, the title compound **48** was obtained after crystallization from MeCN (0.103 g, 35%): m.p. 146−148 °C; IR (KBr): 3442, 3353 (NH), 1638 (NH), 1560, 1533, 1479, 1436 (C=C, C=N), 1291, 1139 (SO_2) cm^{-1}; ^{1}H NMR (500 MHz, DMSO-d_6): δ 2.26 (s, 3H, CH_3), 2.28 (s, 3H, CH_3), 4.38 (s, 2H, SCH_2), 6.39 (s, 1H, H-4 pyrazole), 6.77 (t, 2H, arom.), 6.84 (d, *J* = 7.3 Hz, 2H, arom.), 7.00 (t, 1H, arom.), 7.38 (t, 1H, arom.), 7.42 (s, 1H, H-3), 7.51−7.54 (m, 2H, H-6, arom.), 7.60 (d, *J* = 7.9 Hz, 1H, arom.), 7.70 (s, 1H, arom.), 8.04 (s, 1H, NH), 8.96 (s, 1H, NH) ppm. ^{13}C NMR (125 MHz, DMSO-

d_6): δ 14.1, 19.5, 35.8, 113.1, 124.6, 124.7, 126.2, 126.3, 127.5, 128.0, 128.6, 128.8, 130.1, 131.1, 131.4, 133.2, 133.7, 135.4, 137.9, 138.1, 138.9, 146.6, 151.2, 152.0 ppm; HRMS (ESI-TOF) *m/z* calcd for $C_{26}H_{22}ClF_3N_4O_2S_2$ [M+H$^+$] 579.0898, found 579.0908. Anal. ($C_{26}H_{22}F_3ClN_4O_2S_2$) C, H, N.

*4.1.1.13. N'-{4-Chloro-5-methyl-2-[(4-trifluoromethylphenyl)methylthio]benzenesulfonyl}-1-(5-phenyl-1H-pyrazol-1-yl)amidine (**49**)*

Starting from **25** (0.283 g) with stirring for 1.5 h, the title compound **49** was obtained after crystallization from MeCN (0.082 g, 29%): m.p. 120−123 °C; IR (KBr): 3392 (NH), 1658 (NH), 1567, 1540, 1462, 1431 (C=C, C=N), 1326, 1130 (SO_2) cm^{-1}; ^{1}H NMR (200 MHz, DMSO-*d_6*): δ 2.27 (s, 3H, CH_3), 4.37 (s, 2H, SCH_2), 6.56 (s, 1H, H-4 pyrazole), 6.81−6.84 (m, 2H, arom.), 6.87−6.88 (m, 2H, arom.), 7.03 (t, 1H, arom.), 7.45 (s, 1H, H-3), 7.52 -7.55 (m, 5H, arom., H-6), 7.93 (s, 1H, H-3 pyrazole), 8.20 (s, 1H, NH), 9.20 (s, 1H, NH) ppm; HRMS (ESI-TOF) *m/z* calcd for $C_{25}H_{20}ClF_3N_4O_2S_2$ [M+H$^+$] 565.0741, found 565.0737. Anal. ($C_{25}H_{20}F_3ClN_4O_2S_2$) C, H, N.

*4.1.1.14. N'-{4-Chloro-5-methyl-2-[(4-trifluoromethylphenyl)methylthio]benzenesulfonyl}-1-(3-methyl-5-phenyl-1H-pyrazol-1-yl)amidine (**50**)*

Starting from **26** (0.290 g) with stirring for 1 h, the title compound **50** was obtained after crystallization from MeCN (0.049 g, 17%): m.p. 155−158 °C; IR (KBr): 3450, 3348 (NH), 1651 (NH), 1540, 1509, 1449, 1429 (C=C, C=N), 1323, 1136 (SO_2) cm^{-1}; ^{1}H NMR (500 MHz, DMSO-*d_6*): δ 2.27 (s, 3H, CH_3), 2.29 (s, 3H, CH_3), 4.38 (s, 2H, SCH_2), 6.38 (s, 1H, H-4 pyrazole), 6.78−6.84 (m, 4H, arom.), 7.02 (t, 1H, arom.), 7.42 (s, 1H, H-3), 7.50−7.54 (m, 4H, arom.), 7.56 (s, 1H, H-6), 8.03 (s, 1H, NH), 9.00 (s, 1H, NH) ppm; HRMS (ESI-TOF) *m/z* calcd for $C_{26}H_{22}ClF_3N_4O_2S_2$ [M+H$^+$] 579.0898, found 579.0901. Anal. ($C_{26}H_{22}F_3ClN_4O_2S_2$) C, H, N.

*4.1.1.15. N'-{4-Chloro-2-[(2-chlorophenyl)methylthio]-5-methylbenzenesulfonyl}-1-(5-phenyl-1H-pyrazol-1-yl)amidine (**51**)*

Starting from **27** (0.266 g) with stirring for 4 h, the title compound **51** was obtained after crystallization from EtOH (0.105 g, 39%): m.p. 130−133 °C; IR (KBr): 3417 (NH), 1655 (NH), 1541, 1462, 1425 (C=C, C=N), 1289, 1133 (SO_2) cm^{-1}; ^{1}H NMR (500 MHz, DMSO-*d_6*): δ 2.29 (s, 3H, CH_3), 4.34 (s, 2H, SCH_2), 6.56 (s, 1H, H-4 pyrazole), 6.80 (t, 2H, arom.), 6.96 (d, *J* = 7.3 Hz, 2H, arom.), 7.01 (t, 1H, arom.), 7.20−7.25 (m, 2H, arom.), 7.35 (d, *J* = 7.3

Hz, 1H, arom.), 7.44−7.46 (m, 2H, arom., H-3), 7.54 (s, 1H, H-6), 7.91 (s, 1H, H-3 pyrazole), 8.11 (s, 1H, NH), 9.09 (s, 1H, NH) ppm; HRMS (ESI-TOF) *m/z* calcd for $C_{24}H_{20}Cl_2N_4O_2S_2$ [M+H$^+$] 531.0477, found 531.0428. Anal. ($C_{24}H_{20}Cl_2N_4O_2S_2$) C, H, N.

*4.1.1.16. N'-{4-Chloro-2-[(2-chlorophenyl)methylthio]-5-methylbenzenesulfonyl}-1-(3-methyl-5-phenyl-1H-pyrazol-1-yl)amidine (**52**)*

Starting from **28** (0.273 g) with stirring for 2 h, the title compound **52** was obtained after crystallization from MeCN (0.128 g, 47%): m.p. 135−138 °C; IR (KBr): 3463, 3349 (NH), 1638 (NH), 1558, 1521, 1472, 1446 (C=C, C=N), 1291, 1134 (SO_2) cm^{-1}; ^{1}H NMR (500 MHz, DMSO-d_6): δ 2.29 (s, 6H, 2×CH_3), 4.35 (s, 2H, SCH_2), 6.38 (s, 1H, H-4 pyrazole), 6.78 (t, 2H, arom.), 6,93 (d, *J* = 7.3 Hz, 2H, arom.), 6.99 (t, 1H, arom.), 7.20−7.26 (m, 2H, arom.), 7.35 (d, *J* = 7.3 Hz, 1H, arom.), 7.44−7.46 (m, 2H, arom., H-3), 7.54 (s, 1H, H-6), 7.96 (s, 1H, NH), 8.89 (s, 1H, NH) ppm; HRMS (ESI-TOF) *m/z* calcd for $C_{25}H_{22}Cl_2N_4O_2S_2$ [M+H$^+$] 545.0634, found 545.0612. Anal. ($C_{25}H_{22}Cl_2N_4O_2S_2$) C, H, N.

*4.1.1.17. N'-{4-Chloro-2-[(3-chlorophenyl)methylthio]-5-methylbenzenesulfonyl}-1-(5-phenyl-1H-pyrazol-1-yl)amidine (**53**)*

Starting from **29** (0.266 g) with stirring for 3 h, the title compound **53** was obtained after crystallization from MeCN (0.113 g, 42%): m.p. 124−127 °C; IR (KBr): 3417 (NH), 1655 (NH), 1541, 1462, 1425 (C=C, C=N), 1289, 1133 (SO_2) cm^{-1}; ^{1}H NMR (500 MHz, DMSO-d_6): δ 2.28 (s, 3H, CH_3), 4.27 (s, 2H, SCH_2), 6.59 (s, 1H, H-4 pyrazole), 6.85 (t, 2H, arom.), 6.96 (d, *J* = 7.3 Hz, 2H, arom.), 7.04 (t, 1H, arom.), 7.19−7.28 (m, 3H, arom.), 7.40 (s, 1H, arom.), 7.46 (s, 1H, H-3), 7.49 (s, 1H, H-6), 7.91 (s, 1H, H-3 pyrazole), 8.19 (s, 1H, NH), 9.17 (s, 1H, NH) ppm; HRMS (ESI-TOF) *m/z* calcd for $C_{24}H_{20}Cl_2N_4O_2S_2$ [M+H$^+$] 531.0477, found 531.0454. Anal. ($C_{24}H_{20}Cl_2N_4O_2S_2$) C, H, N.

*4.1.1.18. N'-{4-Chloro-2-[(3-chlorophenyl)methylthio]-5-methylbenzenesulfonyl}-1-(3-methyl-5-phenyl-1H-pyrazol-1-yl)amidine (**54**)*

Starting from **30** (0.273 g) with stirring for 4 h, the title compound **54** was obtained after crystallization from MeCN (0.096 g, 35%): m.p. 108−111 °C; IR (KBr): 3463, 3349 (NH), 1638 (NH), 1558, 1521, 1472, 1446 (C=C, C=N), 1291, 1134 (SO_2) cm^{-1}; ^{1}H NMR (500 MHz, DMSO-d_6): δ 2.27 (s, 3H, CH_3), 2.29 (s, 3H, CH_3), 4.29 (s, 2H, SCH_2), 6.40 (s, 1H, H-4 pyrazole), 6.81 (t, 2H, arom.), 6,91 (d, *J* = 7.3 Hz, 2H, arom.), 7.02 (t, 1H, arom.), 7.20−7.25 (m, 2H, arom.), 7.28 (d, *J* = 7.3 Hz, 1H, arom.), 7.39 (s, 1H, arom.), 7.43 (s, 1H, H-3), 7.51

(s, 1H, H-6), 8.03 (s, 1H, NH), 8.96 (s, 1H, NH) ppm; HRMS (ESI-TOF) *m/z* calcd for $C_{25}H_{22}Cl_2N_4O_2S_2$ [M+H$^+$] 545.0634, found 545.0606. Anal. ($C_{25}H_{22}Cl_2N_4O_2S_2$) C, H, N.

*4.1.1.19. N'-{4-Chloro-2-[(4-chlorophenyl)methylthio]-5-methylbenzenesulfonyl}-1-(5-phenyl-1H-pyrazol-1-yl)amidine (**55**)*

Starting from **31** (0.266 g) with stirring for 2 h, the title compound **55** was obtained after crystallization from MeCN (0.089 g, 33%): m.p. 147−150 °C; IR (KBr): 3446, 3331 (NH), 1648 (NH), 1534, 1491, 1461, 1427 (C=C, C=N), 1291, 1137 (SO_2) cm^{-1}; ^{1}H NMR (500 MHz, DMSO-d_6): δ 2.28 (s, 3H, CH_3), 4.26 (s, 2H, SCH_2), 6.59 (s, 1H, H-4 pyrazole), 6.87 (t, 2H, arom.), 6.95 (d, *J* = 7.3 Hz, 2H, arom.), 7.05 (t, 1H, arom.), 7.23 (d, *J* = 8.3 Hz, 2H, arom.), 7.31 (d, *J* = 8.3 Hz, 2H, arom.), 7.46 (s, 1H, H-3), 7.50 (s, 1H, H-6), 7.93 (s, 1H, H-3 pyrazole), 8.18 (s, 1H, NH), 9.17 (s, 1H, NH) ppm; HRMS (ESI-TOF) *m/z* calcd for $C_{24}H_{20}Cl_2N_4O_2S_2$ [M+H$^+$] 531.0477, found 531.0454. Anal. ($C_{24}H_{20}Cl_2N_4O_2S_2$) C, H, N.

*4.1.1.20. N'-{4-Chloro-2-[(4-chlorophenyl)methylthio]-5-methylbenzenesulfonyl}-1-(3-methyl-5-phenyl-1H-pyrazol-1-yl)amidine (**56**)*

Starting from **32** (0.273 g) with stirring for 1 h, the title compound **56** was obtained after crystallization from MeCN (0.109 g, 40%): m.p. 135−138 °C; IR (KBr): 3457, 3343 (NH), 1648 (NH), 1532, 1508, 1491, 1446, 1422 (C=C, C=N), 1284, 1135 (SO_2) cm^{-1}; ^{1}H NMR (500 MHz, DMSO-d_6): δ 2.27 (s, 3H, CH_3), 2.30 (s, 3H, CH_3), 4.27 (s, 2H, SCH_2), 6.41 (s, 1H, H-4 pyrazole), 6.83 (t, 2H, arom.), 6,91 (d, *J* = 7.8 Hz, 2H, arom.), 7.03 (t, 1H, arom.), 7.22 (d, *J* = 8.3 Hz, 2H, arom.), 7.32 (d, *J* = 8.3 Hz, 2H, arom.), 7.43 (s, 1H, H-3), 7.52 (s, 1H, H-6), 8.01 (s, 1H, NH), 8.97 (s, 1H, NH) ppm; HRMS (ESI-TOF) *m/z* calcd for $C_{25}H_{22}Cl_2N_4O_2S_2$ [M+H$^+$] 545.0634, found 545.0613. Anal. ($C_{25}H_{22}Cl_2N_4O_2S_2$) C, H, N.

*4.1.1.21. N'-[4-Chloro-5-methyl-2-(naphthalene-1-ylmethylthio)benzenesulfonyl]-1-(5-phenyl-1H-pyrazol-1-yl)amidine (**57**)*

Starting from **33** (0.274 g) with stirring for 2 h, the title compound **57** was obtained after crystallization from EtOH (0.148 g, 54%): m.p. 155−158 °C; IR (KBr): 3404, 3309 (NH), 1646 (NH), 1539, 1462, 1427 (C=C, C=N), 1288, 1129 (SO_2) cm^{-1}; ^{1}H NMR (500 MHz, DMSO-d_6): δ 2.29 (s, 3H, CH_3), 4.73 (s, 2H, SCH_2), 6.53 (s, 1H, H-4 pyrazole), 6.74 (t, 2H, arom.), 6.83 (d, *J* = 7.4 Hz, 2H, arom.), 6.97 (t, 1H, arom.), 7.38−7.43 (m, 3H, arom.), 7.46 (s, 1H, H-3), 7.55 (d, *J* = 7.3 Hz, 1H, arom.), 7.67 (s, 1H, H-6), 7.80 (d, *J* = 8.3 Hz, 1H, arom.), 7.83−7.85 (m, 1H, arom.), 7.88 (s, 1H, H-3 pyrazole), 8.10 (s, 1H, NH), 8.15 (d, *J* = 8.8 Hz,

1H, arom.), 9.03 (s, 1H, NH) ppm; HRMS (ESI-TOF) *m/z* calcd for $C_{28}H_{23}ClN_4O_2S_2$ [M+H$^+$] 547.1024, found 545.1030. Anal. ($C_{28}H_{23}ClN_4O_2S_2$) C, H, N.

*4.1.1.22. N'-[4-Chloro-5-methyl-2-(naphthalene-1-ylmethylthio)benzenesulfonyl]-1-(3-methyl-5-phenyl-1H-pyrazol-1-yl)amidine (**58**)*

Starting from **34** (0.281 g) with stirring for 3.5 h, the title compound **58** was obtained after crystallization from EtOH (0.152 g, 54%): m.p. 131−135 °C; IR (KBr): 3424, 3318 (NH), 1643 (NH), 1533, 1507, 1446, 1424 (C=C, C=N), 1287, 1132 (SO_2) cm^{-1}; ^{1}H NMR (500 MHz, DMSO-d_6): δ 2.29 (s, 6H, 2×CH_3), 4.75 (s, 2H, SCH_2), 6.32 (s, 1H, H-4 pyrazole), 6.69 (t, 2H, arom.), 6,75 (d, *J* = 7.8 Hz, 2H, arom.), 6.95 (t, 1H, arom.), 7.37−7.44 (m, 4H, arom. H-3), 7.55 (d, *J* = 6.9 Hz, 1H, arom.), 7.70 (s, 1H, H-6), 7.79 (d, *J* = 8.3 Hz, 1H, arom.), 7.82 (d, *J* = 7.3 Hz, 1H, arom.), 7.92 (s, 1H, NH), 8.14 (d, *J* = 7.8 Hz, 1H, arom.), 8.79 (s, 1H, NH) ppm; HRMS (ESI-TOF) *m/z* calcd for $C_{29}H_{25}ClN_4O_2S_2$ [M+H$^+$] 561.1180, found 561.1187. Anal. ($C_{29}H_{25}ClN_4O_2S_2$) C, H, N.

*4.1.1.23. N'-{4-Chloro-2-[(6-chlorobenzo[d][1,3]dioxol-5-yl)methylthio]-5-methylbenzenesulfonyl}-1-(5-phenyl-1H-pyrazol-1-yl)amidine (**59**)*

Starting from **35** (0.288 g) with stirring for 1 h, the title compound **59** was obtained after crystallization from MeCN (0.157 g, 54%): m.p. 149−152 °C; IR (KBr): 3402, 3307, 3278 (NH), 1654 (NH), 1556, 1542, 1502, 1477, 1464, 1427 (C=C, C=N), 1286, 1135 (SO_2) cm^{-1}; ^{1}H NMR (200 MHz, DMSO-d_6): δ 2.31 (s, 3H, CH_3), 4.25 (s, 2H, SCH_2), 5.98 (s, 2H, OCH_2O), 6.58 (d, *J* = 1.7 Hz, 1H, H-4 pyrazole), 6.78−6.87 (m, 2H, arom.), 6.94−7.08 (m, 5H, arom.)7.47 (s, 1H, H-3), 7.57 (s, 1H, H-6), 7.90 (d, *J* = 1.7 Hz, 1H, H-3 pyrazole), 8.10 (s, 1H, NH), 9.07 (s, 1H, NH) ppm; HRMS (ESI-TOF) *m/z* calcd for $C_{25}H_{20}Cl_2N_4O_4S_2$ [M+H$^+$] 575.0376, found 575.0379. Anal. ($C_{25}H_{20}Cl_2N_4O_4S_2$) C, H, N.

*4.1.1.24. N'-{4-Chloro-2-[(6-chlorobenzo[d][1,3]dioxol-5-yl)methylthio]-5-methylbenzenesulfonyl}-1-(3-methyl-5-phenyl-1H-pyrazol-1-yl)amidine (**60**)*

Starting from **36** (0.295 g) with stirring for 1.5 h, the title compound **60** was obtained after crystallization from MeCN (0.065 g, 22%): m.p. 158−161 °C; IR (KBr): 3442, 3332 (NH), 1642 (NH), 1569, 1534, 1504, 1475, 1449, 1431 (C=C, C=N), 1286, 1134 (SO_2) cm^{-1}; ^{1}H NMR (200 MHz, DMSO-d_6): δ 2.29 (s, 6H, 2×CH_3), 4.26 (s, 2H, SCH_2), 5.97 (s, 2H, OCH_2O), 6.40 (s, 1H, H-4 pyrazole), 6.76−6.83 (m, 2H, arom.), 6.94−7.06 (m, 5H, arom.), 7.44 (s, 1H, H-3), 7.58 (s, 1H, H-6), 7.96 (s, 1H, NH), 8.88 (s, 1H, NH) ppm; HRMS (ESI-

TOF) *m/z* calcd for $C_{26}H_{22}Cl_2N_4O_4S_2$ [M+H$^+$] 589.0532, found 589.0536. Anal. ($C_{26}H_{22}Cl_2N_4O_4S_2$) C, H, N.

4.2. X-ray Structure Determination

Diffraction intensity data were collected on an IPDS 2T dual-beam diffractometer (STOE&Cie GmbH, Darmstadt, Germany) at 120,0(2) K with Mo- Kα_1 radiation of a microfocus x-ray source (GeniX 3D Mo High Flux, 50 kV, 1.0 mA, λ = 0.71073 Å Xenocs, Sassenage, France). The crystal was thermostated in nitrogen stream at 120K using CryoStream-800 device (Oxford CryoSystem, UK) during the entire experiment. Data collection and data reduction were controlled by X-Area 1.75 program [43]. An absorption correction was performed on the integrated reflections by a combination of frame scaling, reflection scaling and a spherical absorption correction. Outliers have been rejected according to Blessing's method [44]. Numerical absorption correction was performed after the optimization of the crystal-shape description by Herrendorf's method [45].

The structures were solved using direct methods with SHELXS-13 program and refined by SHELXL-2014 [46] program run under control of WinGx [47]. All C-H type hydrogen atoms were attached at their geometrically expected positions and refined as riding on heavier atoms with the usual constraints. The N-H hydrogen atoms in Cu-**46** complex were found in the differential Fourier electron density map and were refined without constraints. For **57** N-H bond lengths were constrained to 0.88 Å by using SHELX AFIX 93 instruction.

4.3. Cell Culture and Cell Viability Assay

All chemicals, if not stated otherwise, were obtained from Sigma-Aldrich (St. Louis, MO, USA). The MCF-7 and HeLa cell lines were purchased from Cell Lines Services (Eppelheim, Germany), the HCT-116 cell line was purchased from ATCC (ATCC-No: CCL-247). Cells were cultured in Dulbecco's modified Eagle's medium (DMEM) supplemented with 10% fetal bovine serum, 2 mM glutamine, 100 units/mL penicillin, and 100 µg/mL streptomycin. Cultures were maintained in a humidified atmosphere with 5% CO_2 at 37 °C in an incubator (HeraCell, Heraeus, Langenselbold, Germany).

Cell viability was determined using the MTT (3-(4,5-dimethylthiazol-2-yl)-2,5-diphenyl-tetrazoliumbromide) assay. Stock solutions of the studied compounds were prepared in 100% DMSO. Working solutions were prepared by diluting the stock solutions with DMEM medium, the final concentration of DMSO did not exceed 0.5% in the treated samples. Cells were seeded in 96-well plates at a density of 5×10^3 cells/well and treated for

72 h with the examined compounds in the concentration range 1–100 μM (1, 10, 25, 50 and 100 μM). Following treatment, MTT (0.5 mg/mL) was added to the medium and cells were further incubated for 2 h at 37 °C. Cells were lysed with DMSO and the absorbance of the formazan solution was measured at 550 nm with a plate reader (1420 multilabel counter, Victor, Jügesheim, Germany). The optical density of the formazan solution was measured at 550 nm with a plate reader (Victor 1420 multilabel counter). The experiment was performed in triplicate. Values are expressed as the mean ± SD of at least three independent experiments.

4.4. Cell Cycle Analysis

To determine presence of DNA fragmentation (sub-G1 phase of cell cycle), Hela and HCT 116 cells (1×10^5) were seeded in 1 ml of medium on 24 well plate. After 24 h medium was replaced with fresh one. Then, cells were treated for 24, 48 and 72 h with compound **58** or **60** in the concentration of 50 μM for the indicated times. After treatment cells were collected, washed with PBS and fixed in ice-cold 70% ethanol for 24 h. Then, cells were resuspended in 1 ml of PBS containing RNase A (1 mg/mL) and DAPI (2,5 μg/mL) and incubated for 20 min at room temperature. Samples were analyzed with a flow cytometer (LSRII, Beckton Dickinson).

4.5. Metabolic Stability

Stock solutions of studied compounds were prepared at concentration of 100 mM in DMSO, then thinned down do 100 μM using phosphate buffer. Incubation mixes consisted of 5 μM of studied compound, 100 μM of NADPH in phosphate buffer and 1 mg/ml of pooled human liver microsomes (HLM) (Sigma-Aldrich, St. Louis, MO, USA) in potassium phosphate buffer (0.1 M, pH 7.4). Incubations were carried out in 96-well plates at 37 °C. Incubation mixtures (excluding compound solution) were subjected to 5 minute pre-incubation, and started by addition of 20 μl of compound stock solution. After 0, 5, 10, 15, and 30 minutes 25 μl samples of incubation reaction were added to the equal volume of ice-cold acetonitrile containing 1 μM of internal standard (which was one of the formerly studied amidines, JBS 134). Control incubations were performed without NADPH to assess possible chemical instability. All samples were immediately centrifuged (10 min, 7500 g) and resulted supernatant was directly subjected to LC-MS analysis.

LC-MS analysis was performed on an Agilent 1260 system coupled to SingleQuad 6120 mass spectrometer (Agilent Technologies, Santa Clara, CA, USA). Poroshell C18 EC120 column (3.0 x 100 mm, 2.7 μm, Agilent Technologies, Santa Clara, CA, USA) was used in reversed-phase mode with gradient elution starting with 60% of phase A (0.1% formic acid in deionised water) and 40% of phase B (0.1% formic acid in acetonitrile). Gradient elution program was: 0.00-10.00 min - 40%-100% B; 10.01 min-11.00 min - 100%-40% B; 11.00-15.00 min - 40%B. Total analysis time was 15 min at 40°C, flow rate was 1.0 mL/min and the injection volume was 5 μL. The mass spectrometer was equipped with electrospray ionization source and ionization mode was positive. Mass analyzer was set individually to each derivative to detect pseudomolecular ions [$M+H^+$]. MSD parameters of the ESI source were as follows: nebulizer pressure 35 psig (N_2), drying gas 12 L/min (N_2), drying gas temperature 350 °C, capillary voltage 3.0 kV, fragmentor voltage 150 V.

Acknowledgments

This project was financed by National Science Centre based on the decision number DEC-2013/09/B/NZ7/00048.

Appendix. Supplementary material

Supplementary data associated with this article can be found on the online version at doi:.....

References

[1] International Agency for Research on Cancer. http://globocan.iarc.fr/Pages/fact_sheets_population.aspx, 2012 (accessed 08 February 2018).

[2] U.S. Food and Drug Administration. http://wayback.archive-it.org/7993/20170111064250/http://www.fda.gov/Drugs/InformationOnDrugs/ApprovedDrugs/ucm279174.htm (accessed 08 Feabruary 2018).

[3] J. Mascarenhas, R. Hoffman, Ruxolitinib: the first FDA approved therapy for the treatment of myelofibrosis, Clin. Cancer Res. 18 (2012) 3008−3014.

[4] C. Harrison, A.M. Vannucchi, Ruxolitinib: a potent and selective Janus kinase 1 and 2 inhibitor in patients with myelofibrosis. An update for clinicians, Ther. Adv. Hematol. 3 (2012) 341–354.

[5] G.L. Plosker, Ruxolitinib: a review of its use in patients with myelofibrosis, Drugs. 75 (2015) 297−308.

[6] C.L. O'Bryant, S.D. Wenger, M. Kim, L.A. Thompson, Crizotinib: a new treatment option for ALK-positive non-small cell lung cancer, Ann. Pharmacother. 47 (2013) 189−197.

[7] A. Sahu, K. Prabhash, V. Noronha, A. Joshi, S. Desai, Crizotinib: a comprehensive review, South Asian J. Cancer. 2 (2013) 91–97.

[8] M. Guha, Imbruvica - next big drug in B-cell cancer - approved by FDA, Nat. Biotechnol. 32 (2014) 113−115.

[9] S. Parmar, K. Patel, J.Pinilla-Ibarz, Ibrutinib (Imbruvica): A novel targeted therapy for chronic lymphocytic leukemia, P T. 39 (2014) 483−487.

[10] M. Gross-Goupil, L. François, A. Quivy, A. Ravaud, Axitinib: a review of its safety and efficacy in the treatment of adults with advanced renal cell carcinoma, Clin. Med. Insights Oncol. 7 (2013) 269–277.

[11] T. Tyler, Axitinib: newly approved for renal cell carcinoma, J. Adv. Pract. Oncol. 3 (2012) 333–335.

[12] K. Tzogani, V. Skibeli, I. Westgaard, M. Dalhus, H. Thoresen, K. Bruins Slot, P. Damkier, K. Hofland, J. Borregaard, J. Ersbøll, T. Salmonson, R. Pieters, R. Sylvester, G. Mickisch, J. Bergh, F. Pignattia, The European Medicines Agency approval of axitinib (Inlyta) for the treatment of advanced renal cell carcinoma after failure of prior treatment with sunitinib or a cytokine: summary of the Scientific Assessment of the Committee for Medicinal Products for Human Use, Oncologist. 20 (2015) 20 196–201.

[13] Therapeutic Goods Administration, https://www.tga.gov.au/auspar/auspar-axitinib (accessed 08 Feabruary 2018).

[14] C.O. Ndubaku, T.P. Heffron, S.T. Staben, M. Baumgardner, N. Blaquiere, E. Bradley, R. Bull, S. Do, J. Dotson, D. Dudley, K.A. Edgar, L.S. Friedman, R. Goldsmith, R.A. Heald, A. Kolesnikov, L. Lee, C. Lewis, M. Nannini, J. Nonomiya, J. Pang, S. Price, W.W. Prior, L. Salphati, S. Sideris, J.J. Wallin, L. Wang, B. Wei, D. Sampath, A.G. Olivero, Discovery of 2-{3-[2-(1-isopropyl-3-methyl-1*H*-1,2-4-triazol-5-yl)-5,6-dihydrobenzo[f]imidazo[1,2-d][1,4]oxazepin-9-yl]-1H-pyrazol-1-yl}-2-methylpropanamide (GDC-0032): a β-sparing phosphoinositide 3-kinase inhibitor with high unbound exposure and robust *in vivo* antitumor activity, J. Med. Chem. 56 (2013) 4597−4610.

[15] National Institutes of Health, ClinicalTrials.gov, https://clinicaltrials.gov/ct2/show/NCT02273973, (accessed 08 Feabruary 2018).

[16] National Institutes of Health, ClinicalTrials.gov, https://clinicaltrials.gov/ct2/show/NCT02390427, (accessed 08 Feabruary 2018).

[17] National Institutes of Health, ClinicalTrials.gov, https://clinicaltrials.gov/ct2/show/NCT01862081, (accessed 08 Feabruary 2018).

[18] National Institutes of Health, ClinicalTrials.gov, https://clinicaltrials.gov/ct2/show/NCT02285179, (accessed 08 Feabruary 2018).

[19] National Institutes of Health, ClinicalTrials.gov, https://clinicaltrials.gov/ct2/show/NCT02457910, (accessed 08 Feabruary 2018).

[20] National Institutes of Health, ClinicalTrials.gov, https://clinicaltrials.gov/ct2/show/NCT01296555, (accessed 08 Feabruary 2018).

[21] National Institutes of Health, ClinicalTrials.gov, https://clinicaltrials.gov/ct2/show/NCT02340221, (accessed 08 Feabruary 2018).

[22] National Institutes of Health, ClinicalTrials.gov, https://clinicaltrials.gov/ct2/show/NCT02465060, (accessed 08 Feabruary 2018).

[23] National Institutes of Health, ClinicalTrials.gov, https://clinicaltrials.gov/ct2/show/NCT02785913, (accessed 08 Feabruary 2018).

[24] National Institutes of Health, ClinicalTrials.gov, https://clinicaltrials.gov/ct2/show/NCT02154490, (accessed 08 Feabruary 2018).

[25] A.M. Moilanen, R. Riikonen, R. Oksala, L. Ravanti, E. Aho, G. Wohlfahrt, P.S. Nykänen, O.P. Törmäkangas, J.J. Palvimo, P.J. Kallio, Discovery of ODM-201, a new-generation androgen receptor inhibitor targeting resistance mechanisms to androgen signaling-directed prostate cancer therapies, Sci. Rep. 5 (2015) 12007.

[26] National Institutes of Health, ClinicalTrials.gov, https://clinicaltrials.gov/ct2/show/NCT0279960, (accessed 08 Feabruary 2018).

[27] National Institutes of Health, ClinicalTrials.gov, https://clinicaltrials.gov/ct2/show/NCT02200614, (accessed 08 Feabruary 2018).

[28] National Institutes of Health, ClinicalTrials.gov, https://clinicaltrials.gov/ct2/show/NCT03004534, (accessed 08 Feabruary 2018).

[29] M.S. Squires, R.E. Feltell, N.G. Wallis, E.J. Lewis, D.M. Smith, D.M. Cross, J.F. Lyons, N.T. Thompson, Biological characterization of AT7519, a small-molecule inhibitor of cyclin-dependent kinases, in human tumor cell lines, Mol. Cancer Ther. 8 (2009) 324−332.

[30] National Institutes of Health, ClinicalTrials.gov, https://clinicaltrials.gov/ct2/show/NCT02503709, (accessed 08 Feabruary 2018).

[31] National Institutes of Health, ClinicalTrials.gov, https://clinicaltrials.gov/ct2/show/NCT00390117, (accessed 08 Feabruary 2018).

[32] https://clinicaltrials.gov/ct2/show/NCT01627054, (accessed 08 Feabruary 2018).

[33] National Institutes of Health, ClinicalTrials.gov, https://clinicaltrials.gov/ct2/show/NCT01652144, (accessed 08 Feabruary 2018).

[34] J. Sławiński, K. Brożewicz, A. Fruziński, M.L. Główka, synthesis and antitumor activity of novel *N'*-(2-benzylthiobenzenesulfonyl)-1*H*-pyrazole-1-amidine derivatives, Heterocycles 83 (2011) 1093−1109.

[35] B. Żołnowska, J. Sławiński, K. Szafrański, A. Angeli, C.T. Supuran, A. Kawiak, M. Wieczór, J. Zielińska, T. Bączek, S. Bartoszewska, Novel 2-(2-arylmethylthio-4-chloro-5-methylbenzenesulfonyl)-1-(1,3,5-triazin-2-ylamino)guanidine derivatives: inhibition of human carbonic anhydrase cytosolic isozymes I and II and the transmembrane tumor-associated isozymes IX and XII, anticancer activity, and molecular modeling studies, Eur. J. Med. Chem. 143 (2018) 1931−1941.

[36] B. Żołnowska, J. Sławiński, A. Pogorzelska, K. Szafrański, A. Kawiak, G. Stasiłojć, M. Belka, J. Zielińska, T. Bączek, Synthesis, QSAR studies, and metabolic stability of novel 2-alkylthio-4-chloro-*N*-(5-oxo-4,5-dihydro-1,2,4-triazin-3-yl)benzenesulfonamide derivatives as potential anticancer and apoptosis-inducing agents, Chem. Biol. Drug Des. 90 (2017) 380−396.

[37] A. Pogorzelska, J. Sławiński, B. Żołnowska, K. Szafrański, A. Kawiak, J. Chojnacki, S. Ulenberg, J. Zielińska, T. Bączek, Novel 2-(2-alkylthiobenzenesulfonyl)-3-(phenylprop-2-ynylideneamino)guanidine derivatives as potent anticancer agents : synthesis, molecular structure, QSAR studies and metabolic stability, Eur. J. Med. Chem. 138 (2017) 357−370.

[38] J. Sławiński, K. Szafrański, A. Pogorzelska, B. Żołnowska, A. Kawiak, K. Macur, M. Belka, T. Bączek, Novel 2-benzylthio-5-(1,3,4-oxadiazol-2-yl)benzenesulfonamides with anticancer activity: synthesis, QSAR study, and metabolic stability, Eur. J. Med. Chem. 132 (2017) 236−248.

[39] B. Żołnowska, J. Sławiński, A. Pogorzelska, K. Szafrański, A. Kawiak, G. Stasiłojć, M. Belka, S. Ulenberg, T. Bączek, J. Chojnacki, Novel 5-substituted 2-(aylmethylthio)-4-chloro-*N*-(5-aryl-1,2,4-triazin-3-yl)benzenesulfonamides: synthesis, molecular structure, anticancer activity, apoptosis-inducing activity and metabolic stability, Molecules 21 (2016) 808.

[40] B. Żołnowska, J. Sławiński, M. Belka, T. Bączek, A. Kawiak, J. Chojnacki, A. Pogorzelska, K. Szafrański, Synthesis, molecular structure, metabolic stability and QSAR

studies of a novel series of anticancer *N*-acylbenzenesulfonamides, Molecules 20 (2015) 19101−19129.

[41] J. Sławiński, P. Bednarski, R. Grünert, P. Reszka, Syntheses of a new series of *N*-amino-*N′′*-(benzenesulphonyl)guanidine derivatives with potential antitumor activity, Polish J. Chem. 77 (2003) 53–64.

[42] J. Sławiński, A. Pogorzelska, B. Żołnowska, A. Kędzia, M. Ziółkowska-Klinkosz, E. Kwapisz, Synthesis and anti-yeast evaluation of novel 2-alkylthio-4-chloro-5-methyl-*N*-[imino-(1-oxo-(1*H*)-phthalazin-2-yl)methyl]benzenesulfonamide derivatives, Molecules 19 (2014) 13704–13723.

[43] STOE & Cie GmbH (2015). X-Area 1.75, software package for collecting single-crystal data on STOE area-detector diffractometers, for image processing, scaling reflection intensities and for outlier rejection; Darmstadt, Germany.

[44] R.H. Blessing, Outlier Treatment in Data Merging, J. Appl. Cryst. 30 (1997) 421 – 426.

[45] W. Herrendorf, HABITUS, a program for the optimization of the crystal description for the numerical absorption correction by means of suitable, psi scanned reflections; dissertation 1994, Karlsruhe; extension 1998, Gießen, Germany.

[46] G.M. Sheldrick, Crystal structure refinement with SHELX, Acta Cryst. C71 (2015) 3−8.

[47] L.J. Farrugia, WinGX and ORTEP for Windows: an update J. Appl. Cryst. 45 (2012) 849−854.

New series of 2-mercaptobenzenesulfonamides have been synthesized.

HCT-116 and HeLa cell lines were the most susceptible for tested compounds.

Four compounds display 4-fold higher activity against HeLa than HaCaT cells.

Active compounds cause DNA fragmentation in HCT-116 and HeLa cells.